The Free Internet Journal
for Organic Chemistry

Paper

Archive for
Organic Chemistry

Arkivoc **2020**, part iii, 0-0
to be inserted by editorial office

Synthesis, structural elucidation, intramolecular hydrogen bonding and DFT studies of quinoline-chalcone-chromene hybrids

Lamla Thungatha, Saba Alapour, and Neil A. Koorbanally*

School of Chemistry and Physics, University of KwaZulu-Natal, Private Bag X54001, Durban, 4001, South Africa
Email: Koorbanally@ukzn.ac.za

Received 03-12-2020 **Accepted** 07-31-2020 **Published on line** 08-12-2020

Abstract

Eight hydroxyquinoline-chromene chalcones, of which six were new, were synthesized using the Vilsmeier-Haack reaction and Claisen-Schmidt condensation. These contain either mono or dichromene functionality. The hydroxyl proton chemical shift of both types of compounds at varying temperature indicated weakened hydrogen bonds with an increase in temperature, however there was no significant difference to the slopes of the OH chemical shift curves (3.4 x10^{-3} for the 2-methoxychromene derivative and 3.1 x10^{-3} for the 6-methoxydichromene derivative. Potential energy scans of these two compounds were obtained using B3LYP/6-311 G level theory in the gas phase, and showed the enol form to be most stable for both molecules and that the energy barrier to make proton transfer possible is 5.076 and 3.989 Kcal mol^{-1} for the 2-methoxychromene and 6-methoxydichromene derivatives respectively.

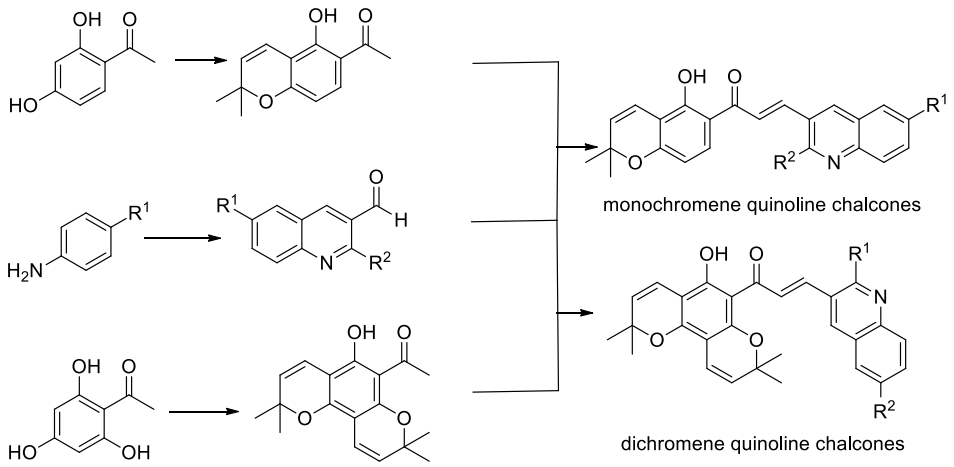

Keywords: Quinoline, chalcones, chromenes, molecular hybrids, DFT studies, hydrogen bonding

DOI: https://doi.org/10.24820/ark.5550190.p011.193

Introduction

Quinoline is a heterocyclic aromatic organic molecule with a broad spectrum of pharmacological properties including antimalarial,[1] antibacterial,[2-3] antifungal,[4] anticancer,[5] antitubercular,[6] antileishmanial[7] and anti-inflammatory.[8] Current pharmaceuticals containing this pharmacophore include Amodiaquine, Chloroquine, Ciprofloxacin, Levofloxacin and Mefloquine. These drugs have a quinoline core hybridised with other pharmacophores leading to more potent drugs. Quinoline molecules substituted at C-3 are also known for their broad range of biological activities. These hybrid molecules include quinoline chalcones synthesised from 3-quinoline carbaldehydes and have shown promising anticancer,[5] antibacterial[9] and antiprotozoal[10] activities. Quinoline chalcones are also used as precursors for bioactive quinoline pyrazole derivatives.[11]

Benzopyran on the other hand, consists of a benzene ring fused to a pyran ring and is mostly found in natural products. They show a broad range of biological activities, such as anticancer[12] and anti-inflammatory activity.[13] This scaffold also forms part of the flavones, potent antioxidants and known to have good biological activity.[14]

Derivatives of *ortho*-hydroxy acetophenone, used to synthesise chalcones are known to have intramolecular hydrogen bonding (IHB) and intramolecular proton transfer (IPT) properties.[15] Intramolecular proton transfer is also known to be enhanced by photoexcitation of the molecule. This concept is known as the excited state intramolecular proton transfer (ESIPT) and was first studied by Albert Weller.[16] IHB and IPT or ESIPT have since been extensively studied both theoretically and experimentally.[17] The two phenomena occur by interaction of the oxygen atom of the carbonyl group C=O and the hydrogen atom of the hydroxy group in 2-hydroxyacetophenones. IHB and ESIPT are known to affect the physical properties of the molecule as well as their bioactivity, photochemistry and reactivity, which differ depending on the properties of the molecular subunits or core structure.[18-20] The chalcones reported in this work have a hydroxyl group on the chromene core adjacent to the carbonyl carbon of the chalcone.

The hydrogen bond is an important intermolecular interaction in biochemical processes.[21] NMR chemical shifts are very sensitive to steric, electronic effects, and molecular interactions.[22] It is therefore a good tool to identify and study hydrogen bond interactions. Hydrogen bonds are classified in two different groups, strong and weak hydrogen bonds. Strong hydrogen bonds are those in which hydrogen is covalently bound to N, O, or F and form a second weak interaction to another electronegative atom (N, O, or F).[23] Weak hydrogen bonding is when hydrogen is attached to a sp^x (x = 1–3) hybridized carbon and forms additional weak interactions with electronegative atoms.[24-25] In a weak hydrogen bond, the hydrogen bond donor must be electron deficient enough to be attracted to an electron-rich atom.[25]

We herein report the synthesis of quinoline chromenochalcone hybrid molecules, their structural elucidation by NMR, and a study of the hydrogen bonding using VT NMR. DFT studies, carried out to understand the electronic properties of the molecule are also reported.

Results and Discussion

The quinoline-3-carbaldehyde intermediates (**1**) were synthesised in three steps using the Vilsmeier-Haack reaction where $POCl_3$ and DMF were reacted with acetanilides (Scheme 1).[26-28] The chromene derivatives were made in a single step, which involved reaction of 2,4-dihydroxy or 2,4,6-trihydroxyacetophenone with 3-methylcrotonaldehyde to form the desired monochromene (**2**) or dichromene (**3**) acetophenone derivatives.

The final step involved reaction of the quinoline-3-carbaldehydes with the chromeno acetophenones using the Claisen-Schmidt condensation[29] to synthesise quinoline chromenochalcone hybrids (**4**).

The Vilsmeier-Haack reaction works better in dry conditions and the Claisen-Schmidt condensation does not work well with some hydroxyacetophenones,[30-31] indicated by the low yields of **4a-h** (38-46%). This can be attributed to the competing enolate ion and phenoxide ion of the hydroxyacetophenone arising from the base abstraction of both the α proton and hydroxy proton of the acetophenone.[32]

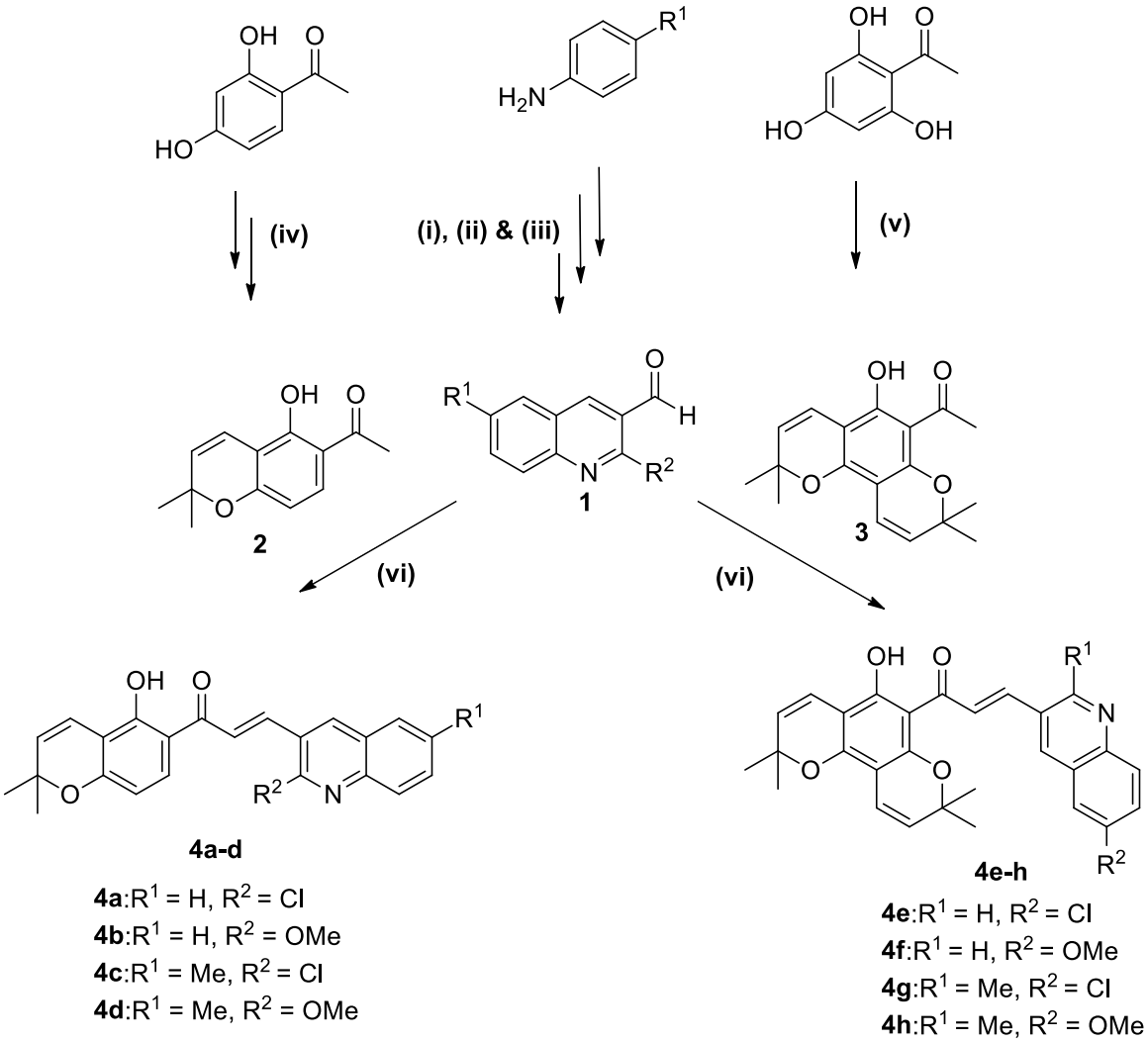

Scheme 1. Synthetic scheme to quinoline chromenochalcones. (i) Acetic anhydride, 6 h; (ii) DMF, $POCl_3$, 80 °C, 18 h; (iii) MeOH, KOH reflux; (iv) 3-methylcrotonaldehyde (1 eq.), pyridine, 150 °C, 12 h; (v) 3-methylcrotonaldehyde (2 eq.), pyridine, 150 °C, 12 h; (vi) KOH, EtOH, rt, 48 h.

Characteristic resonances for all chalcones were observed. For example in **4f**, the two doublets for H-9 and H-10 occured at δ 7.97 and 8.27 respectively with large coupling constants of 15.8 Hz, an indication of *trans* coupled alkene protons. The formation of these compounds was also confirmed by HMBC correlations of H-9 to C-2 and C-4, and H-10 to C-3. The *α,β*-unsaturated carbonyl resonance occurred at δ193.1. The chromene rings are characterised by a pair of doublets for each ring (H-10' and H-11' at δ5.47 and δ6.61, and H-3' and H-4' at δ5.47 and δ6.69) and two methyl resonances at δ1.45 (H-2a'/H-2b') and δ1.54 (H-9a' and H-9b'). The resonances for each of the pairs of olefinic protons in the chromene rings were paired in the COSY spectrum.

Furthermore, H-9a' and H-9b' showed HMBC correlations to C-10', and H-2a' and H-2b' showed HMBC correlations to C-3'. H-4' and H-3' showed HMBC correlations to C-8a' and C-4a' respectively (Figure 1). The hydroxyl proton H-5a' also showed a correlation to C-4a' confirming the assignment of this system. Both methyl resonances of the chromene ring adjacent to the hydroxyl group showed NOESY correlations to the hydroxyl proton H-5a'.

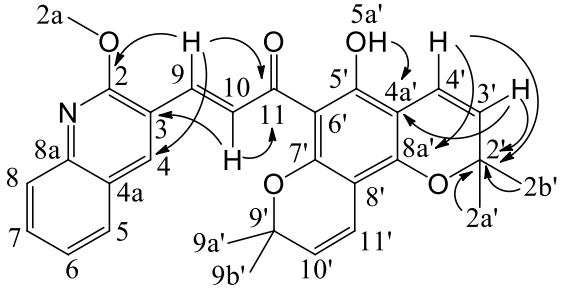

Figure 1. Selected HMBC correlations for **4f.**

The proton resonances of H-4 to H-8 on the quinoline ring were observed to be more deshielded when a chloro group was substituted at C-2 than when a methoxy group was substituted at the same position. This is attributed to the more electronegative chloro group, withdrawing electron density from the quinoline ring as opposed to the electron donating methoxy group. With the hydroxy proton 5a', the opposite occurs. Compounds with a chloro group have a more shielded proton resonance for H-5a' than those compounds with a chloro group. This is indicative of slightly weaker hydrogen bonding between the hydroxy group and carbonyl group of the *α,β*-unsaturated moiety (the stronger the hydrogen bonding, the more deshielded the resonance is) as opposed to when a methoxy is situated at the same position. This is possibly due to the slightly shorter C=O bond due to the electronegative chloro group. As usual, the *β* proton, H-9 in the chalcone moiety is more deshielded than H-10 due to resonance effects.[33] These correlations are later confirmed in the 3D crystal and DFT optimised structures. The ^{13}C NMR data is fairly consistent across the series of compounds.

The synthesised compounds formed crystals by slow evaporation in a solution of ethanol. Single crystal X-ray diffraction data for **4b** and **4f** (with atom numbering shown in Figure 2 below) show that **4b** is monoclinic and **4f** triclinic with space group P21/n and P-1 respectively. In **4b**, an intramolecular hydrogen bond is observed between the hydroxyl proton H2 and the carbonyl oxygen O3 (1.754 Å) and between the same atoms in **4f** between H2 and O5 (1.708 Å) (Figures 2 and 3). The reason for the stronger hydrogen bond when a second ring is added to the structure is not known, but could involve the additional oxygen present in **4f**. Intermolecular hydrogen bonds are also observed with the methyl groups, nitrogen in the quinoline ring and oxygen in the hydroxy and methoxy groups and in the chromene ring (Table 1). In **4b**, the monochromeno chalcone (Figure 2), the quinoline ring is situated with the methoxy group (O4-C24) and the nitrogen (N5) *trans* to the carbonyl group (C12-O3). This situates the two electronegative oxygen atoms as far apart as possible. However, in **4f**, the dichromenochalcone (Figure 3), the quinoline ring rotates itself 180° (compared to **4b**) around the C9-C10 bond, due to steric hindrance, so as to move out of the way of the dimethyl groups (C-29 and C-30) and the pyran oxygen (O4) in the angular pyran ring. The methoxy group (O3-C22) and nitrogen (N1) is now situated *cis* to the carbonyl group (C7-O5).

Table 1. Intermolecular hydrogen bonds for **4b** and **4f**

Compound **4b**		Compound **4f**	
D-H…A	d(H…A)/Å	D-H…A	d(H…A)
C(24)-H(24b)…O(1)	2.561	C(1)-H(1c)…N(1)	2.694
C(4)-H(4)…O(3)	2.715	C(15)-H(15a)…N(1)	2.704
C(2)-H(2b)…O(3)	2.704	C(29)-H(29a)…O(5)	2.484
		C(29)-H(29b)…O(2)	2.680
		C(30)-H(30c)…O(3)	2.526

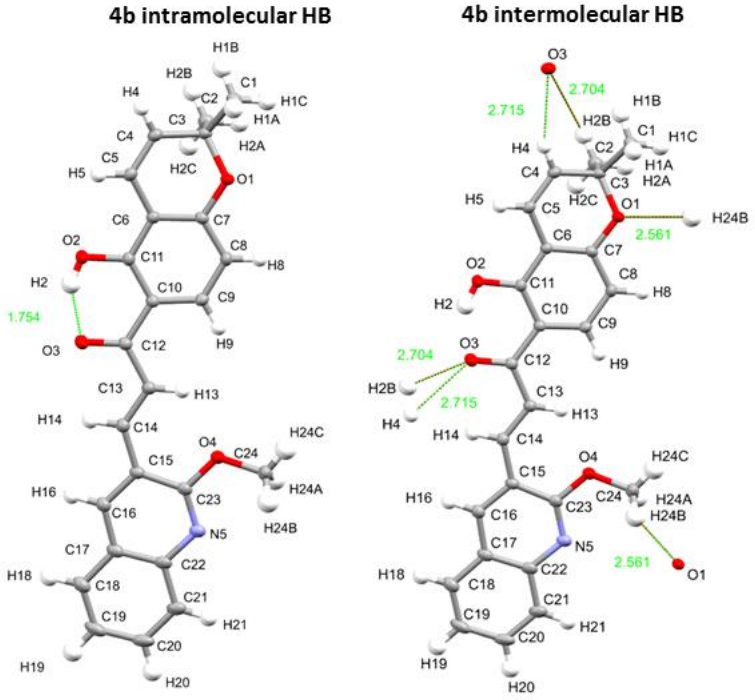

Figure 2. Intramolecular and intermolecular hydrogen bonds for **4b.**

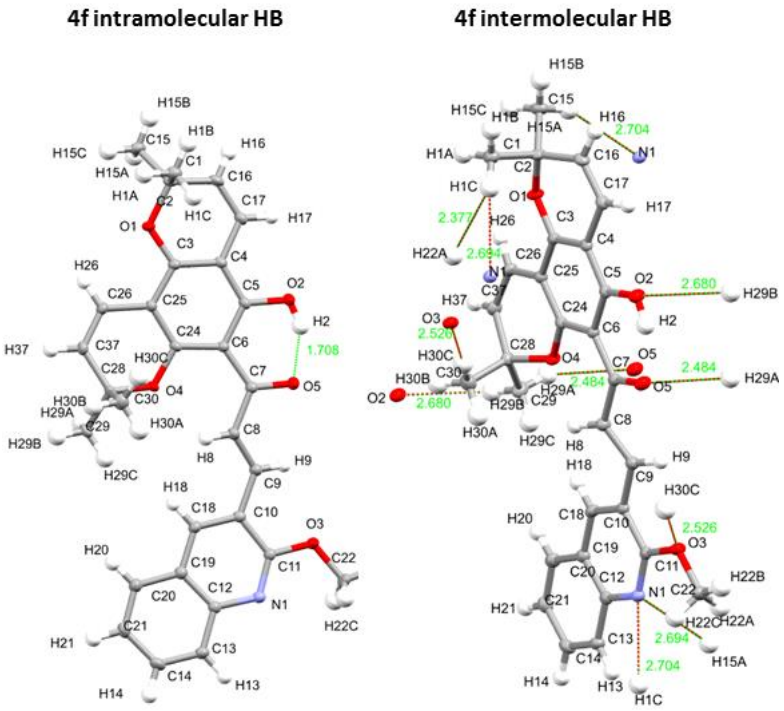

Figure 3. Intramolecular and intermolecular hydrogen bonds for **4f.**

Variable Temperature NMR studies

Hydrogen bonding of the O-H proton H-5a' (Figure 1) with the carbonyl oxygen at C-11 was indicated by the downfield chemical shift between δ 13.47-14.30, and further suggested by a broad O-H stretching band at 2489-2637 cm^{-1} in the IR spectrum. Compounds **4b** with a single pyran ring and **4f** with two pyran rings were selected to study the strength of the hydrogen bond at different temperatures. Compound **4f** with an O-H chemical shift at δ 14.30 at room temperature was more deshielded than **4b** δ 13.68 indicating that the extra pyran ring affected hydrogen bonding in some way. The strength of the hydrogen bond in solution can be determined by chemical shift variation of a proton in the hydrogen bond donor.[23, 34]

The chemical shift of the O-H proton decreased linearly with increasing temperature for both compounds indicating weakening of hydrogen bond interactions with increasing temperature (Figure S40). However, the slopes of the two compounds **4b** (3.4 $x10^{-3}$ ppm/K) and **4f** (3.1 $x10^{-3}$ ppm/K) did not show a significant difference, 13.47-13.70 ppm for **4b** and 14.10-14.30 ppm for **4f**. This indicates that this hydrogen bond in both compounds were fairly strong and not disrupted by additional heat.

In **4b**, the H-9 chemical shift decreases (becomes more shielded) non-linearly with an increase in temperature (Figure S12), due to a weakening of the H bond. The opposite is observed in **4f** (Figure S36), where the quinoline ring is rotated 180° around the C3-C9 bond compared to **4b** (Figure 1). In this case, an increase in chemical shift is experienced with increase in temperature, due to H-9 being in close proximity to both the oxygen atoms of the methoxy and carbonyl groups.

Frontier molecular orbitals and photophysical properties of the molecule

Good agreement in bond lengths and angles between the single crystal X-ray data and DFT calculations were observed. This indicated that theoretical calculations were a good approximation of the observed values. It also indicated that solid and gas phase structures are similar. HOMO-LUMO energy values and their band gaps

were obtained for structures **4a-h** (Figure 4). The charge distribution of frontier molecular orbitals follows the same trend. Essentially, the HOMO electron density is mostly distributed on the chromene or dichromene core and the LUMO electron density on the quinoline core and partially on the benzene ring of the chromene or dichromene core. The band gaps of the chromene derivatives (**4a-4d**) are observed to be higher ~3.2 eV compared to the dichromene derivatives (**4e-4h**), which is ~2.9 eV. Band gaps are known to be related to stability of the molecule. The larger the band gap, the more stable the molecule, indicating the greater stability of the chromene derivative over their dichromene counterparts.

Molecular electrostatic potential (MEP) maps assigns electrostatic potential on each atom of the molecule. This phenomenon correlates with dipole moment, electronegativity and partial charges,[35] and makes it possible to identify reactive sites of a molecule toward nucleophiles and electrophiles. One can also see how charge distribution of the molecule can affect inter- and intramolecular interactions. The red shaded portions indicate negative regions, reactive to electrophiles and the blue shaded portions are positive, reactive to nucleophiles.[36] Figure 5 shows that the 2-hydroxy and carbonyl oxygen atoms are the most electronegative, being the best electron bond acceptors in the molecule. This results in intramolecular hydrogen bonding between the O-H proton and carbonyl group oxygen and intermolecular hydrogen bonding between the O-H oxygen and hydrogen bond donors in adjacent molecules.

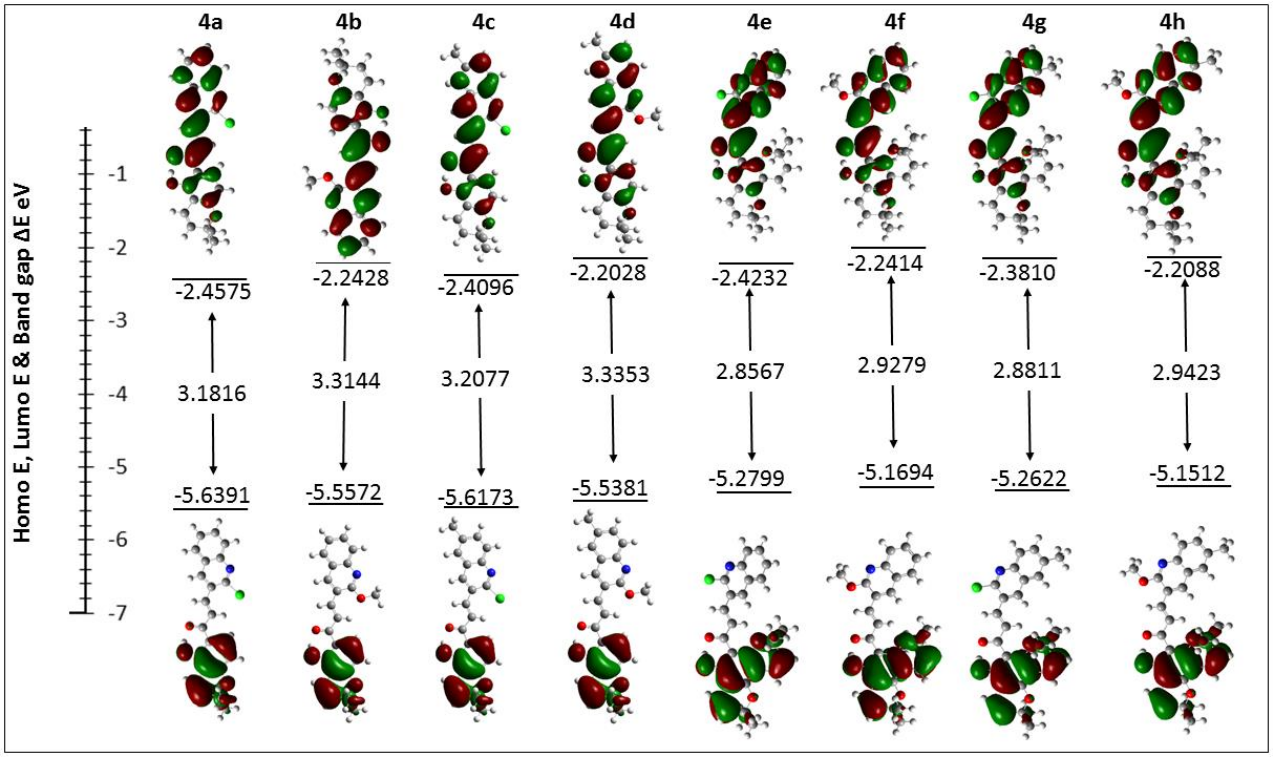

Figure 4. Frontier molecular orbitals and energies for **4b** and **4f** in chloroform.

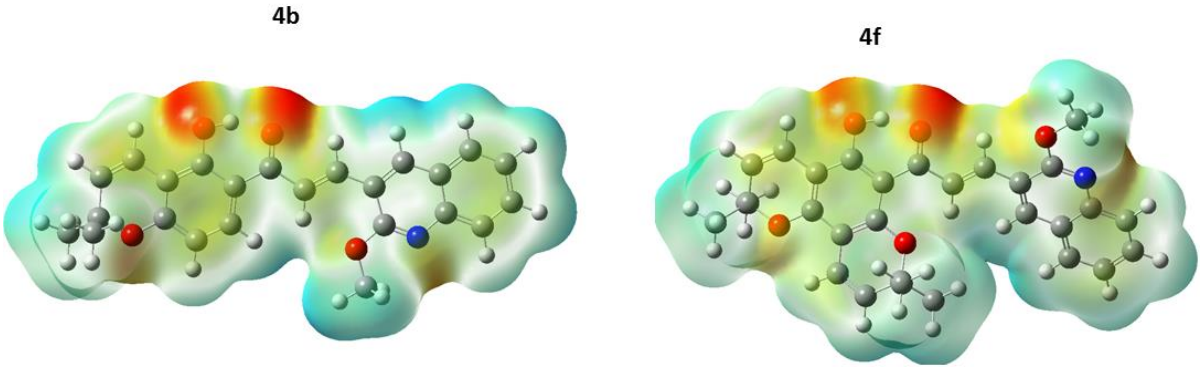

Figure 5. MEP plots for compound **4b** and **4f** in chloroform.

To understand the intramolecular proton transfer of **4b** and **4f**, the relaxed potential energy scans of the optimised molecules were carried out (Figure 6) using B3LYP/6-311 ++G (d, p) level theory in the gas phase. This involved varying the redundant internal coordinates of the O-H bond from 0.9-1.7 Å, with increment steps of 0.05 Å. The method was set to optimize the structures at each increment step and perform single point calculations. The energies were obtained for each bond length of O-H fixed at 0.9-1.7 Å with increment steps of 0.05 Å. The curve compares the two molecules. Both have the same global minimum, the enol form, which is the most stable form for both molecules. A slight bend in the curves is observed, which seems to correspond to local minima. The two molecules show different relative energies at this point 5.076 and 3.989 Kcal/mol for **4b** and **4f** respectively. These points estimate the energy barrier required to make proton transfer possible. This means it is easier for **4f** to undergo proton transfer and form the ketone than **4b**, indicating greater hydrogen bonding in **4f**, corroborating the discussion made earlier.

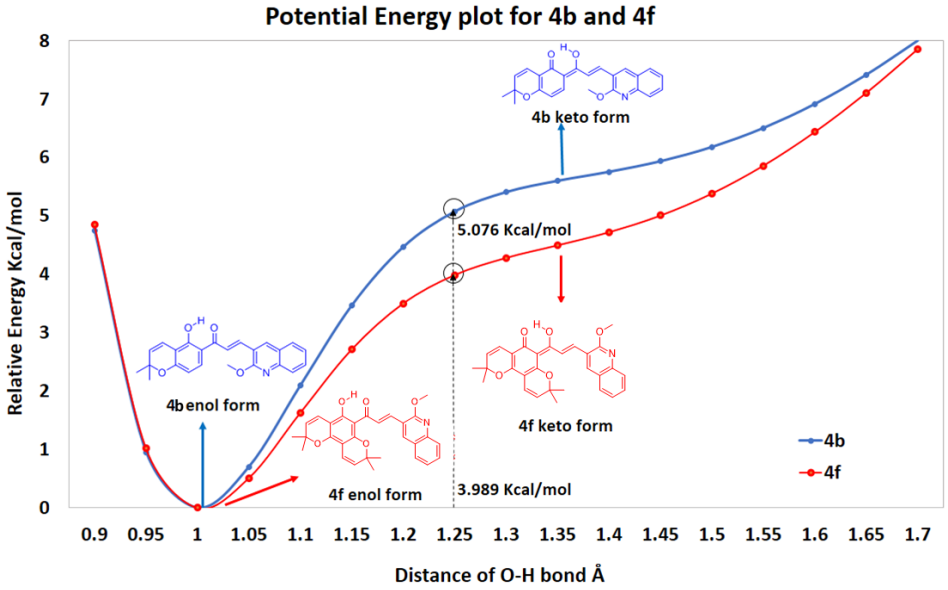

Figure 6. Potential energy plot for **4b** and **4f** in chloroform.

UV-VIS spectra of all compounds indicate two absorption maxima at 263-280 nm and 359-373 nm, corresponding to π–π* and n-π* transitions respectively (Figure 7).[37] Compounds **4a-d** have a stronger absorption intensity at ~ 359-373 nm (n-π*), while **4e-h** have a stronger absorption intensity at ~ 263-280 nm

(π–π*). This is due to extra conjugation brought about by the extra chromene ring in the dichromene derivatives.

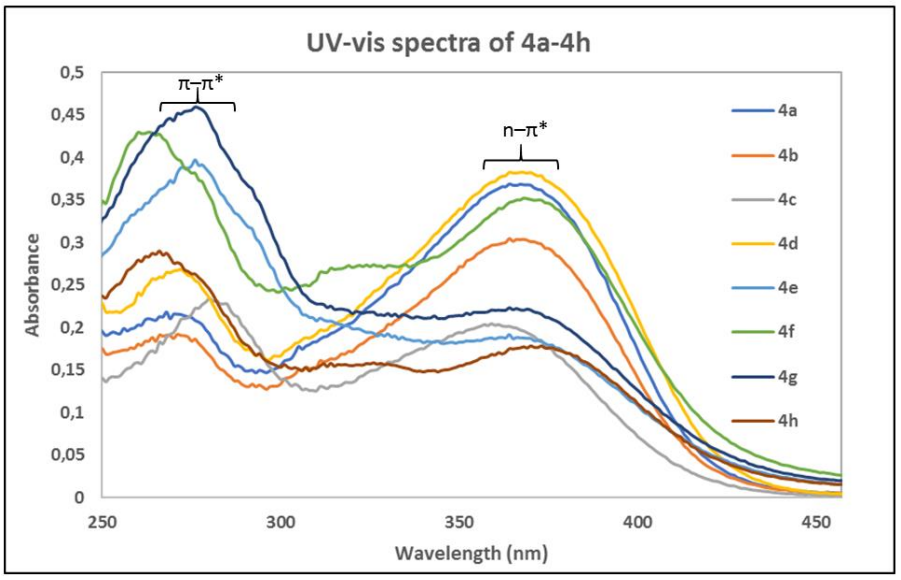

Figure 7. Overlaid UV-VIS spectra for **4a-h.**

Conclusions

The hydroxy quinoline-chromene chalcones were successfully synthesised and analysed using spectral techniques. The presence of hydrogen bonding was initially confirmed by the OH chemical shift of the compounds. The structural difference of the chromene and dichromene derivatives resulted in observed differences in the ^{1}H NMR chemical shift of the OH proton. Intramolecular hydrogen bonding was shown to respond to varying temperature. The O-H proton of both derivatives were observed to shift upfield upon temperature increase, with slightly different slopes. The potential energy scans further confirm that these molecules are stable in the enol form. The HOMO-LUMO band gaps suggest that the dichromene derivatives are less stable. The structural difference of the two derivatives result in an observable effect of the electronic and physical parameters of the molecule.

Experimental Section

General. Chemicals were purchased from Sigma-Aldrich, South Africa. Thin layer chromatography and column chromatography were performed using Kieselgel 60 F_{254} plates and silica gel (60-120 mesh) respectively with hexane, dichloromethane, ethyl acetate and methanol in various ratios as the mobile phase. All solvents were dried and redistilled according to standard procedures. Melting points were determined on an Electrothermal IA9100 melting point apparatus. Infrared data was recorded on a Perkin Elmer Spectrum 100 FT-IR spectrometer with universal attenuated total reflectance sampling accessory. Ultraviolet spectra were obtained on a Shimadzu UV-VIS spectrophotometer in ethanol. High-resolution mass data was obtained using a Waters Micromax LCT Premier TOF-MS instrument, operating at ambient temperatures, with a sample

concentration of approximately 1 ppm. ^{1}H and ^{13}C NMR spectra were recorded at 298 K with 5 to 10 mg samples dissolved in 0.5 mL of $CDCl_3$ in 5-mm NMR tubes using a Bruker Avance 400-MHz NMR spectrometer (9.4 T; Bruker, Germany) (400.22 MHz for ^{1}H, 100.63 MHz for ^{13}C and 376.58 Hz for ^{19}F). The FID resolution was 0.501 Hz/pt for ^{1}H and 0.734 Hz/pt for ^{13}C spectra. Chemical shifts are reported in ppm and coupling constants (*J*) in Hz. ^{1}H and ^{13}C NMR spectra were referenced to the solvent line of 7.24 and 77.0, respectively for deuterated chloroform.

Synthesis

Acetanilides Acetanilides were prepared according to the procedure of Dulla et al.[38] Aniline or *p*-toluidine (15 mmol) was added to a round bottomed flask containing acetic anhydride (21 mmol) and the reaction stirred at room temperature for 30 min. Upon completion, the contents were poured in ice water, where white or creamy precipitates were filtered and recrystallized in water.

2-Chloro-3-formylquinolines (1a and 1b). A modified method of Meth-Cohn et al. [39] was used. Briefly, freshly dried DMF (33.5 mmol) was transferred to a dry round bottomed flask fitted with a condenser attached to a drying tube. $POCl_3$ (93.8 mmol) was added dropwise to the DMF at 0-5 °C for 10-15 min. After addition, the reaction was stirred for 20 min and the acetanilide (13.4 mmol) added. The reaction was stirred at 80-90 °C for 12-16 h. On completion, the reaction mixture was cooled to room temperature and poured in ice water. A golden yellow precipitate was filtered and recrystallized in ethyl acetate.

2-Methoxy-3-formylquinolines (1c and 1d). A modified method of Waghray et al.[40] was used. Briefly, the 2-chloro-3-formylquinolines **1a** (10.4 mmol) and **1b** (10.4 mmol) were added to a solution of potassium hydroxide (15.6 mmol) in methanol (100 mL) and the contents refluxed overnight. Upon completion, the reaction was cooled to room temperature and cold water added to precipitate the product, which was then filtered and dried.

1-(5-Hydroxy-2,2-dimethyl-2*H*-chromen-6-yl)ethanone (2). The method of Gupta et al.[41] was employed with modification. 2,4-Dihydroxyacetophenone (5.00 g, 32.90 mmol) was added to a solution of dry pyridine (3.50 mL) followed by 3-methyl-but-2-enal (3.20 mL, 32.90 mmol). The contents were refluxed for 4 hours at 110 °C, after which an equivalent amount of 3-methyl-but-2-enal (3.20 mL, 32.90 mmol) was added to the reaction mixture. The reaction was then refluxed overnight. The product was then dissolved in ethyl acetate and purified by column chromatography on silica gel using ethyl acetate and hexane (3:7).

1-(5-Hydroxy-2,2,8,8-tetramethyl-2,8-dihydropyrano[2,3-f]chromen-6-yl)ethanone (3). The method outlined in Pawar and Koorbanally[42] was followed. 3-Methyl-but-2-enal (4.70 mL, 47.6 mmol) was added to a stirred solution of 2,4,6-trihydroxyacetophenone (2.00 g, 11.9 mmol) in dry pyridine (1.37 mL). The reaction was stirred at 110 °C overnight. After the reactant was completely consumed, the solvent was evaporated and the thick brown paste purified by column chromatography on silica gel using ethyl acetate and hexane (1:9).

Quinoline chromenochalcones (4a-d) and quinoline dichromenochalcones (4e-h). The method reported by Lee and Kim[43] was adapted. The quinoline aldehyde **1** (1.04 mmol) and chromene **2** or dichromene **3** (0.86 mmol) was added to a solution of potassium hydroxide (8.70 mmol) in ethanol (8.00 mL). The reaction was stirred at room temperature for 48 h. Upon completion, the contents were poured in cold water and

neutralised with HCl. The resultant precipitate was filtered and dried. The product was purified by column chromatography using 5% ethyl acetate in hexane as the mobile phase.

(*E*)-3-(2-Chloroquinolin-3-yl)-1-(5-hydroxy-2,2-dimethyl-2*H*-chromen-6-yl)prop-2-en-1-one (4a). Yellow crystalline solid; yield 40%; mp 156-157 °C; IR (neat, ν_{max}, cm^{-1}) 1700 (C=O); λ_{max} (log ε): 271 (4.27), 367 (4.51); ^{1}H NMR (400 MHz, $CDCl_3$) δ_H 1.46 (6H, s, H-2a'/H-2b'), 5.59 (1H, d, *J* 10.1 Hz, H-3'), 6.39 (1H, d, *J* 8.8 Hz, H-8'), 6.74 (1H, d, *J* 10.1 Hz, H-4'), 7.59 (1H, ddd, J_1 8.6 Hz, J_2 7.4 Hz, J_3 1.0 Hz, H-6), 7.66 (1H, d, *J* 15.5 Hz, H-10), 7.72 (1H, d, *J* 8.8 Hz, H-7'), 7.77 (1H, ddd, J_1 8.4 Hz, J_2 7.3 Hz, J_3 1.0 Hz, H-7), 7.87 (1H, d, *J* 8.1, H-5), 8.02 (1H, d, *J* 8.4 Hz, H-8), 8.25 (1H, d, *J* 15.5 Hz, H-9), 8.47 (1H, s, H-4), 13.47 (1H, s, H-5a'); ^{13}C NMR (100 MHz, $CDCl_3$) δ_C 28.4 (C-2a'/C-2b'), 78.1 (C-2'), 108.6 (C-8'), 109.5 (C-4a'), 113.9 (C-6'), 115.7 (C-4'), 124.8 (C-10), 127.0 (C-4a), 127.8 (C-6), 128.0 (C-5), 128.1 (C-3), 128.3 (C-3'), 128.5 (C-8), 130.8 (C-7'), 131.7 (C-7), 136.3 (C-4), 138.8 (C-9), 147.9 (C-8a), 150.4 (C-2), 160.3 (C-8'a), 161.1 (C-5'), 191.0 (C-11).

(*E*)-1-(5-Hydroxy-2,2-dimethyl-2*H*-chromen-6-yl)-3-(2-methoxyquinolin-3-yl)prop-2-en-1-one (4b). Yellow crystalline solid; yield 43%; mp 152–153 °C; IR (neat, ν_{max}, cm^{-1}) 1630 (C=O); λ_{max} (log ε): 271 (4.26), 364 (4.56); ^{1}H NMR (400 MHz, $CDCl_3$) δ_H 1.46 (6H, s, H-2a'/ H-2b'), 4.18 (3H, s, H-2a), 5.58 (1H, d, *J* 10.4 Hz, H-3'), 6.39 (1H, d, *J* 8.9 Hz, H-8'), 6.75 (1H, d, *J* 10.4 Hz, H-4'), 7.38 (1H, ddd, J_1 8.3 Hz, J_2 7.7 Hz, J_3 1.5 Hz, H-6), 7.63 (1H, ddd, J_1 8.3 Hz, J_2 7.4 Hz, J_3 1.1 Hz, H-7), 7.73 (1H, d, *J* 8.9 Hz, H-7'), 7.75 (1H, d, *J* 8.3 Hz, H-5), 7.83 (1H, d, *J* 8.3 Hz, H-8), 7.87 (1H, d, *J* 15.8 Hz, H-10), 8.06 (1H, d, *J* 15.8 Hz, H-9), 8.24 (1H, s, H-4), 13.68 (1H, s, H-5a'); ^{13}C NMR (100 MHz, $CDCl_3$) δ_C 28.4 (C-2a'/C-2b'), 53.9 (C-2a), 77.9 (C-2'), 108.4 (C-8'), 109.4 (C-4a'), 114.2 (C-6'), 115.9 (C-4'), 120.2 (C-3), 123.5 (C-10), 124.7 (C-6), 125.0 (C-4a), 127.1 (C-8) 128.0 (C-5), 128.2 (C-3'), 130.8 (C-7, C-7'), 138.7 (C-9), 139.1 (C-4), 146.9 (C-8a), 160.0 (C-2), 160.2 (C-8a'), 161.1 (C-5'), 192.1 (C-11); HRMS (neg) *m/z* 386.1398 [M-H] (calcd. for $C_{24}H_{20}NO_4$: 386.1392).

(*E*)-3-(2-Chloro-6-methylquinolin-3-yl)-1-(5-hydroxy-2,2-dimethyl-2*H*-chromen-6-yl)prop-2-en-1-one (4c). Yellow crystalline solid; yield 38%; mp 189-191 °C; IR (neat, ν_{max}, cm^{-1}) 1631 (C=O); λ_{max} (log *ε*): 280 (4.36), 359 (4.30); ^{1}H NMR (400 MHz, $CDCl_3$) δ_H 1.46 (6H, s, H-2a'/H-2b'), 2.53 (3H, s, H-6a), 5.59 (1H, d, *J* 10.0 Hz, H-3'), 6.39 (1H, d, *J* 8.9 Hz, H-8'), 6.74 (1H, d, *J* 10.0 Hz, H-4'), 7.58 (1H, dd, J_1 8.6 Hz, J_2 1.8 Hz, H-7), 7.62 (1H, s, H-5), 7.63 (1H, d, *J* 15.4 Hz, H-10), 7.71 (1H, d, *J* 8.9 Hz, H-7'), 7.89 (1H, d, *J* 8.6 Hz, H-8), 8.23 (1H, d, *J* 15.4 Hz, H-9), 8.36 (1H, s, H-4), 13.48 (1H, s, H-5a'); ^{13}C NMR (100 MHz, $CDCl_3$) δ_C 21.6 (C-6a), 28.4 (C-2a'/C-2b'), 78.1 (C-2'), 108.6 (C-8'), 109.5 (C-4a'), 113.9 (C-6'), 115.8 (C-4'), 124.5 (C-10), 126.8 (C-5), 127.0 (C-4a), 127.8 (C-3), 128.1 (C-8), 128.3 (C-3'), 130.8 (C-7'), 134.0 (C-7), 135.7 (C-4), 137.9 (C-6), 139.0 (C-9), 146.6 (C-8a), 160.3 (C-8a'), 161.1(C-5'), 191.0 (C-11); HRMS (neg) *m/z* 404.1049 [M-H] (calcd. for $C_{24}H_{19}NO_3Cl$ 404.1053).

(*E*)-1-(5-Hydroxy-2,2-dimethyl-2*H*-chromen-6-yl)-3-(2-methoxy-6-methylquinolin-3-yl)prop-2-en-1-one (4d). Yellow crystalline solid; yield 40%; mp 150-151 °C; IR (neat, ν_{max}, cm^{-1}) 1633 (C=O); λ_{max} (log *ε*): 272 (4.38), 367 (4.53); ^{1}H NMR (400 MHz, $CDCl_3$) δ_H 1.46 (6H, s, H2a'/H-2b'), 2.47 (3H, s, H-6a), 4.15 (3H, s, H-2a), 5.58 (1H, d, *J* 10.2 Hz, H-3'), 6.38 (1H, d, *J* 9.0 Hz, H-8'), 6.74 (1H, d, *J* 10.2 Hz, H-4'), 7.46 (1H, dd, J_1 8.5 Hz, J_2 1.9 Hz, H-7), 7.49 (1H, s, H-5), 7.71 (2H, d, *J* 9.0 Hz, H-7', H-8), 7.85 (1H, d, *J* 15.6 Hz, H-10), 8.02 (1H, d, *J* 15.6 Hz, H-9), 8.13 (1H, s, H-4), 13.70 (1H, s, H-5a'); ^{13}C NMR (100 MHz, $CDCl_3$) δ_C 21.3 (C-6a), 28.4 (C-2a'/C-2b'), 53.8 (C-2a), 77.9 (C-2'), 108.3 (C-8'), 109.4 (C-4a'), 114.2 (C-6'), 115.9 (C-4'), 120.0 (C-3), 123.3 (C-10), 125.0 (C-4a), 126.8 (C-8), 127.0 (C-5), 128.1 (C-3'), 130.8 (C-7'), 132.9 (C-7), 134.3 (C-6), 138.7 (C-4), 138.9 (C-9), 145.2 (C-8a), 159.8 (C-8a'), 159.9 (C-2), 161.0 (C-5'), 192.2 (C-11); HRMS (neg) *m/z* 400.1541 [M-H] (calcd. for $C_{25}H_{22}NO_4$ 400.1549).

(*E*)-3-(2-Chloroquinolin-3-yl)-1-(5-hydroxy-2,2,8,8-tetramethyl-2*H*,8*H*-pyrano[2,3-*f*]chromen-6-yl)prop-2-en-1-one (4e). Brown crystalline solid; Yield 45%; mp 215-217 °C; IR (neat) ν_{max} 1639 cm^{-1} (C=O); λ_{max} (log *ε*): 276 (4.66), 364 (4.34); ^{1}H NMR (400 MHz, $CDCl_3$) δ_H 1.45 (6H, s, H-2a'/H-2b'), 1.53 (6H, s, H-9a'/H-9b'), 5.47 (1H, d, *J* 10.0 Hz, H-10'), 5.48 (1H, d, *J* 10.0 Hz, H-3'), 6.61 (1H, d, *J* 10.0 Hz, H-11'), 6.68 (1H, d, *J* 10.0 Hz, H-4'), 7.58

(1H, ddd, J_1 8.1 Hz, J_2 7.7 Hz, J_3 0.9 Hz, H-6), 7.75 (1H, ddd, J_1 8.4 Hz, J_2 7.7 Hz, J_3 1.5 Hz, H-7), 7.81 (1H, d, *J* 8.1 Hz, H-5), 8.02 (1H, d, *J* 8.4 Hz, H-8), 8.13 (1H, d, *J* 15.5 Hz, H-9), 8.19 (1H, d, *J* 15.5, H-10), 8.41 (1H, s, H-4), 14.14 (1H, s, H-5a'); ^{13}C NMR (100 *MHz*, $CDCl_3$) δ_C 28.1 (C-2a'/C-2b'), 28.5 (C-9a'/C-9b'), 78.5 (C-2', C-9'), 102.0 (C-4a', C-8'), 105.8 (C-6'), 116.1 (C-4'), 116.6 (C-11'), 124.8 (C-10'), 125.6 (C-3'), 127.2 (C-4a), 127.6 (C-6), 127.8 (C-5), 128.5 (C-8), 128.9 (C-3), 131.4 (C-7), 131.9 (C-10), 135.7 (C-4), 136.2 (C-9), 147.7 (C-8a), 150.6 (C-2), 155.6 (C-8a'), 156.9 (C-7'), 161.6 (C-5'), 191.9 (C-11); HRMS (neg) *m/z* 472.1324 [M-H] (calcd. for $C_{28}H_{23}NO_4Cl$ 472.1316).

(*E*)-1-(5-Hydroxy-2,2,8,8-tetramethyl-2*H*,8*H*-pyrano[2,3-*f*]chromen-6-yl)-3-(2-methoxyquinolin-3-yl)prop-2-en-1-one (4f). Brown crystalline solid; yield 42%; mp 178-180 °C; IR (neat, ν_{max}, cm^{-1}) 1700 (C=O); λ_{max} (log ε): 263 (4.58), 368 (4.27); ^{1}H NMR (400 MHz, $CDCl_3$) δ_H 1.45 (6H, s, H-2a'/H-2b'), 1.54 (6H, s, H-9a'/H-9b'), 4.16 (3H, s, H-2a), 5.47 (2H, d, *J* 10.0 Hz, H-3', H-10'), 6.61 (1H, d, *J* 10.0 Hz, H-11'), 6.69 (1H, d, *J* 10.0 Hz, H-4'), 7.38 (1H, ddd, J_1 8.0 Hz, J_2 7.5 Hz, J_3 1.2 Hz, H-6), 7.63 (1H, ddd, J_1 8.5 Hz, J_2 7.5 Hz, J_3 1.2 Hz, H-7), 7.71 (1H, d, *J* 8.0 Hz, H-5), 7.83 (1H, d, *J* 8.5 Hz, H-8), 7.97 (1H, d, *J* 15.8 Hz, H-9), 8.21 (1H, s, H-4), 8.27 (1H, d, *J* 15.8, H-10), 14.30 (1H, s, H-5a'); ^{13}C NMR (100 MHz, $CDCl_3$) δ_C 27.9 (C-9a'/C-9b'), 28.4 (C-2a'/C-2b'), 53.9 (C-2a), 78.3 (C-9'), 78.4 (C-2'), 102.6 (C-4a', C-8'), 106.1 (C-6'), 116.3 (C-4'), 116.6 (C-11'), 121.0 (C-3), 124.6 (C-6), 124.9 (C-10'), 125.2 (C-4a), 125.4 (C-3'), 127.0 (C-8), 127.9 (C-5), 130.5 (C-7), 130.7 (C-10), 136.2 (C-9), 138.1 (C-4), 146.7 (C-8a), 155.4 (C-8a'), 156.2 (C-7'), 160.3 (C-2), 161.4 (C-5'), 193.1 (C-11); HRMS (neg) *m/z* 468.1821 [M-H] (calcd. for $C_{30}H_{22}NO_5$ 468.1824).

(*E*)-3-(2-Chloro-6-methylquinolin-3-yl)-1-(5-hydroxy-2,2,8,8-tetramethyl-2*H*,8*H*-pyrano[2,3-*f*]chromen-6-yl)prop-2-en-1-one (4g). Brown crystalline solid; Yield 46%; mp 189-190 °C; IR (neat, ν_{max}, cm^{-1}) 1700 (C=O); λ_{max} (log ε): 276 (4.60), 369 (4.51); ^{1}H NMR (400 MHz, $CDCl_3$) δ_H 1.45 (6H, s, H-2a'/H-2b'), 1.53 (6H, s, H-9a'/H-9b'), 2.53 (3H, s, H-6a), 5.48 (1H, d, *J* 10.0 Hz, H-3'), 5.49 (1H, d, *J* 10.0 Hz, H-10'), 6.61 (1H, d, *J* 10.0 Hz, H-11'), 6.68 (1H, d, *J* 10.0 Hz, H-4'), 7.54 (1H, s, H-5), 7.57 (1H, dd, J_1 8.4, J_2 1.8 Hz, H-7), 7.90 (1H, d, *J* 8.4 Hz, H-8), 8.11 (1H, d, *J* 15.7 Hz, H-9), 8.16 (1H, d, *J* 15.7 Hz, H-10), 8.31 (1H, s, H-4), 14.16 (1H, s, H-5a'); ^{13}C NMR (100 MHz, $CDCl_3$) δ_C 21.6 (C-6a), 28.2 (C-9a'/C-9b'), 28.5 (C-2a'/C-2b'), 78.5 (C-2', C-9'), 102.6 (C-8'), 102.7 (C-4a'), 105.9 (C-6'), 116.1 (C-4'), 116.6 (C-11'), 124.8 (C-10'), 125.5 (C-3'), 126.6 (C-5), 127.2 (C-4a), 128.2 (C-8), 128.7 (C-3), 131.6 (C-10), 133.7 (C-7), 135.1 (C-4), 136.4 (C-9), 137.7 (C-6), 146.4 (C-8a), 149.7 (C-2), 155.7 (C-8a'), 156.2 (C-7'), 161.5 (C-5'), 191.9 (C-11); HRMS (neg) *m/z* 482.1975 [M-H] (calcd. for $C_{30}H_{28}NO_5$ 482.1967).

(*E*)-1-(5-Hydroxy-2,2,8,8-tetramethyl-2*H*,8*H*-pyrano[2,3-*f*]chromen-6-yl)-3-(2-methoxy-6-methylquinolin-3-yl)prop-2-en-1-one (4h). Brown crystalline solid; yield 43%; mp 148-149 °C; IR (neat, ν_{max}, cm^{-1}) 1700 (C=O); λ_{max} (log ε): 266 (4.66), 373 (4.34); ^{1}H NMR (400 MHz, $CDCl_3$) δ_H 1.44 (6H, s, H-2a'/H-2b'), 1.54 (6H, s, H9a'/H-9b'), 2.48 (3H, s, H-6a), 4.13 (3H, s, H-2a), 5.47 (2H, d, *J* 10.0 Hz, H-3', H-10'), 6.61 (1H, d, *J* 10.0 Hz, H-11'), 6.68 (1H, d, *J* 10.0 Hz, H-4'), 7.46 (1H, dd, J_1 8.6, J_2 1.6 Hz, H-7), 7.47 (1H, s, H-5), 7.72 (1H, d, *J* 8.6 Hz, H-8), 7.97 (1H, d, *J* 16.0 Hz, H-9), 8.12 (1H, s, H-4), 8.23 (1H, d, *J* 16.0 Hz, H-10), 14.31 (1H, s, H-5a'); ^{13}C NMR (100 MHz, $CDCl_3$) δ_C 21.3 (C-6a), 28.0 (C-9a'/C-9b'), 28.4 (C-2a'/C-2b'), 53.8 (C-2a), 78.3 (C-2'/C-9'), 102.5 (C-4a'), 102.6 (C-8'), 106.1 (C-6'), 116.3 (C-4'), 116.6 (C-11'), 120.8 (C-3), 124.9 (C-10'), 125.1 (C-4a), 125.4 (C-3'), 126.7 (C-8), 126.9 (C-5), 130.5 (C-10), 132.7 (C-7), 134.2 (C-6), 136.6 (C-9), 137.7 (C-4), 145.1 (C-8a), 155.4 (C-8a'), 156.2 (C-7'), 159.9 (C-2), 161.4 (C-5'), 193.2 (C-11); HRMS (neg) *m/z* 482.1961 [M-H] (calcd. for $C_{30}H_{28}NO_5$ 482.1967).

Computational studies

The 2D structure of the synthesized molecular hybrids **6a-6l** were prepared using ChemBioDraw Ultra 13.0 and optimized using DFT with B3LYP at 6-31G (d, p) level basis sets.[44-46] For intramolecular hydrogen bonding calculations, compounds **4b** and **4f** were further optimized using 6-311G (d, p).[47] The harmonic vibrational frequency calculations of the optimised molecules were evaluated at the same level of theory as optimisation

and the absence of imaginary frequencies confirmed that the stationary points obtained correspond to the true minima of the potential energy surface. Symmetry of the molecules was not specified in all calculations. Software default convergence parameters were used and the optimisations carried out in the gaseous phase. Calculations were carried out using Gaussian 09 A.02 and visualized using Gauss View 5.0.8 software.[48-49] The final optimised 3D structures were used to obtain frontier molecular orbitals, HOMO-LUMO energies and molecular electrostatic potential (MEP) plots. Potential energy scans were determined for **4b** and **4f** to investigate the potential energy barrier of the intramolecular proton transfer of the OH proton and its effect on molecular structure.

Single crystal X-ray diffraction analysis

The compounds were dissolved in methanol and allowed to slowly crystallise at room temperature. Crystal structures of **4b** and **4f** were determined on a Bruker Smart APEX II diffractometer with Mo Kα radiation. Data reduction was carried out using the System Administrator's Integrated Network Tool (SAINT+). SHELXS was used to solve and refine the structure. Hydrogen atoms were positioned geometrically and refined isotropically. Crystallographic images were prepared using Mercury 3.9. Crystallographic data has been deposited with the Cambridge Crystallographic Data Centre, CCDC, 12 Union Road, Cambridge CB21EZ, UK. Copies of the data can be obtained free of charge on quoting the depository numbers CCDC-1895603 and 1895604 (Fax: +44-1223-336-033; E-Mail: deposit@ccdc.cam.ac.uk http://www.ccdc.cam.ac.uk).

Acknowledgements

NK thanks the National Research Foundation South Africa for a Competitive Grant for Rated Researchers (Grant No. 118534) and Incentive Funding for Rated Researchers (Grant No. 114817), and the CSIR Armscor Ledger Grant for research costs and a bursary for Lamla Thungatha.

Supplementary Material

^{1}H and ^{13}C NMR data, High Resolution Mass spectra and graphs depicting the changes in the ^{1}H NMR chemical shifts of certain resonances as a function of temperature can be found in the supplementary material file.

References

1. Kaur, K.; Jain, M.; Reddy, R.P.; Jain, R. *Eur. J. Med. Chem.* **2010**, *45*, 3245. https://doi.org/10.1016/j.ejmech.2010.04.011
2. Marella, A.; Tanwar, O.P.; Saha, R.; Ali, M.R.; Srivastava, S.; Akhter, M.; Shaquiquzzaman, M.; Alam, M.M. *Saudi Pharm. J.* **2013**, *21*, 1. https://doi.org/10.1016/j.jsps.2012.03.002
3. Garudachari, B.; Isloor, A. M.; Satyanarayana, M.N.; Fun, H.-K.; Hegde, G. *Eur. J. Med. Chem.* **2014**, *74*, 324. https://doi.org/10.1016/j.ejmech.2014.01.008
4. Duval, A.R.; Carvalho, P.H.; Soares, M.C.; Gouvêa, D.P.; Siqueira, G.M.; Lund, R.G.; Cunico, W. *ScientificWorldJournal* **2011**, *11*, 1489.

https://doi.org/10.1100/tsw.2011.141
5. Afzal, O.; Kumar, S.; Haider, M.R.; Ali, M.R.; Kumar, R.; Jaggi, M.; Bawa, S. *Eur. J. Med. Chem.* **2015**, *97*, 871. https://doi.org/10.1016/j.ejmech.2014.07.044
6. Candéa, A.L.P.; Ferreira, M.D.L.; Pais, K.C.; Cardoso, L.N.D.F.; Kaiser, C.R.; Henriques, M.D.G.M.D.O.; Lourenço, M.C.S.; Bezerra, F.A.F.M.; Souza, M.V.N.D. *Bioorg. Med. Chem. Lett.* **2009**, *19*, 6272. https://doi.org/10.1016/j.bmcl.2009.09.098
7. Gopinath, V.S.; Rao, M.; Shivahare, R.; Vishwakarma, P.; Ghose, S.; Pradhan, A.; Hindupur, R.; Sarma, K.D.; Gupta, S.; Puri, S.K.; Launay, D.; Martin, D. *Bioorg. Med. Chem. Lett.* **2014**, *24*, 2046. https://doi.org/10.1016/j.bmcl.2014.03.065
8. El-Feky, S.A.H.; El-Samii, Z.K.A.; Osman, N.A.; Lashine, J.; Kamel, M.A.; Thabet, H.K. *Bioorg. Chem.* **2015**, *58*, 104. https://doi.org/10.1016/j.bioorg.2014.12.003
9. Garrison, A.T.; Abouelhassan, Y.; Yang, H.; Yousaf, H.H.; Nguyen, T.J.; Huigens III, R.W. *MedChemComm*, **2017**, *8*, 720. https://doi.org/10.1039/C6MD00381H
10. Ramírez-Prada, J.; Robledo, S.M.; Vélez, I.D.; Crespo, M.D.P.; Quiroga, J.; Abonia, R.; Montoya, A.; Svetaz, L.; Zacchino, S.; Insuasty, B. *Eur. J. Med. Chem.* **2017**, *131*, 237. https://doi.org/10.1016/j.ejmech.2017.03.016
11. Nikam, M.D.; Mahajan, P.S.; Damale, M.G.; Sangshetti, J.N.; Dabhade, S.K.; Shinde, D.W.; Gill, C.H. *Med. Chem. Res.* **2015**, *24*, 3372. https://doi.org/10.1007/s00044-015-1385-x
12. Wang, L.; Chen, G.; Lu, X.; Wang, S.; Han, S.; Li, Y.; Ping, G.; Jiang, X.; Li, H.; Yang, J.; Wu, C. *Eur. J. Med. Chem.* **2015**, *89*, 88. https://doi.org/10.1016/j.ejmech.2014.10.036
13. Wei, Z.; Yang, Y.; Xie, C.; Li, C.; Wang, G.; Ma, L.; Xiang, M.; Sun, J.; Wei, Y.; Chen, L. *Fitoterapia* **2014**, *97*, 172. https://doi.org/10.1016/j.fitote.2014.06.002
14. Dinesh, K.; Pooja, S.; Harmanpreet, S.; Kuna, N.; Girish Kumar, G.; Subheet Kumar, J.; Fidele, N.K. *RSC Advances* **2017**, *7*, 36977. https://doi.org/10.1039/C7RA05441F
15. Filarowski, A.; Koll, A.; Kochel, A.; Kalenik, J.; Hansen, P.E. *J. Mol. Struct.* **2004**, *700*, 67. https://doi.org/10.1016/j.molstruc.2004.01.033
16. Weller, A. *Z. Electrochem., Ber Bunsenges Phys Chem.* **1956**, *60*, 1144.
17. Sobczyk, L.; Chudoba, D.; Tolstoy, P.M.; Filarowski, A. *Molecules* **2016**, *21*, 1657. https://doi.org/10.3390/molecules21121657
18. Kanaani, A.; Ajloo, D.; Ghasemian, H.; Kiyani, H.; Vakili, M.; Mosallanezhad, A. *Struct. Chem.* **2015**, *26*, 1095. https://doi.org/10.1007/s11224-015-0571-2
19. Li, C.; Li, D.; Ma, C.; Liu, Y. *J. Mol. Liq.* **2016**, *224*, 83. https://doi.org/10.1016/j.molliq.2016.09.088
20. Li, H.; Yin, H.; Liu, X.; Shi, Y. *J. At. Mol. Sci.* **2016**, 7, 115-124.
21. Mitchell, J.B.O.; Price, S.L. *J. Comput. Chem.* **1990**, *11*, 1217. https://doi.org/10.1002/jcc.540111014

22. Charisiadis, P.; Kontogianni, V.G.; Tsiafoulis, C.G.; Tzakos, A.G.; Siskos, M.; Gerothanassis, I.P. *Molecules* **2014**, *19*, 13643. https://doi.org/10.3390/molecules190913643
23. Taylor, R. *Cryst. Growth Des.* **2016**, *16*, 4165. https://doi.org/10.1021/acs.cgd.6b00736
24. Desiraju, G.R. *Acc. Chem. Res.* **1996**, *29*, 441. https://doi.org/10.1021/ar950135n
25. Alkorta, I.; Elguero, J. *Chem. Soc. Rev.* **1998**, *27*, 163. https://doi.org/10.1039/a827163z
26. Rajput, A.P.; Rajput, S.S. *Int. J. Pharm. Pharm. Sci.* **2011**, *3*, 346.
27. Rani, K.M.; Rajendran, S.P. *Int. J. Innovative Res. Sci. Eng. Technol.* **2014**, *3*, 15966.
28. Venkanna, P.; Rajanna, K.C.; Satish Kumar, M.; Ansari, M.B.; Moazzam Ali, M. *Tetrahedron Lett.* **2015**, *56*, 5164.
29. Abonia, R.; Insuasty, D.; Castillo, J.; Insuasty, B.; Quiroga, J.; Nogueras, M.; Cobo, J. *Eur. J. Med. Chem.* **2012**, *57*, 29. https://doi.org/10.1016/j.ejmech.2012.08.039
30. Kulkarni, P.; Swami, P.; Zubaidha, P. *Synth. React. Inorg., Met.-Org., Nano-Met. Chem.* **2013**, *43*, 617. https://doi.org/10.1080/15533174.2012.752392
31. Khan, K.; Siddiqui, Z.N. *Appl. Organomet. Chem.* **2014**, *28*, 789. https://doi.org/10.1002/aoc.3200
32. Patil, C.B.; Mahajan, S.K.; Katti, S.A. *J. Pharm. Sci. Res.* **2009**, *1*, 11.
33. Moodley, T.; Momin, M.; Mocktar, C. Kannigadu, C., Koorbanally, N. A. *Magn. Reson. Chem.* **2016**, *54*, 610. https://doi.org/10.1002/mrc.4414
34. Alapour, S.; Farahani, M.D.; Silva, J.R.A.; Alves, C.N.; Friedrich, H.B.; Ramjugernath, D.; Koorbanally, N. A. *Monatsh. Chem.* **2017**, *148*, 2061. https://doi.org/10.1007/s00706-017-2044-3
35. Gandhimathi, S.; Balakrishnan, C.; Venkataraman, R.; Neelakantan, M.A. *J. Mol. Liq.* **2016**, *219*, 239. https://doi.org/10.1016/j.molliq.2016.02.097
36. Alphonse, R.; Varghese, A.; George, L.; Nizam, A. *J. Mol. Liq.* **2016**, *215,* 387. https://doi.org/10.1016/j.molliq.2015.12.050
37. Li, Q.; Li, B.; Liu, B.; Yu, M. *J. Chem. Res.* **2010**, *34*, 379. https://doi.org/10.3184/030823410X12780936189898
38. Dulla, B., Vijayavardhini, S., Rambau, D., Anuradha, V., Rao, M., Pal, M. *Curr. Green Chem.* **2014**, *1*, 73. https://doi.org/10.2174/2213346114019990002
39. Meth-Cohn, O.; Narine, B.; Tarnowski, B. *Tetrahedron Lett.* **1979**, *20*, 3111. https://doi.org/10.1016/S0040-4039(01)95334-1
40. Waghray, D.; Zhang, J.; Jacobs, J.; Nulens, W.; Basarić, N.; Meervelt, L.V.; Dehaen, W. *J. Org. Chem.* **2012**, *77*, 10176. https://doi.org/10.1021/jo301814m
41. Gupta, S.; Shivahare, R.; Korthikunta, V.; Singh, R.; Gupta, S.; Tadigoppula, N. *Eur. J. Med. Chem.* **2014**, *81*, 359. https://doi.org/10.1016/j.ejmech.2014.05.034
42. Pawar, S.S.; Koorbanally, N.A. *Magn. Reson. Chem.* **2014**, *52***,** 279. https://doi.org/10.1002/mrc.4062

43. Lee, Y.R.; Kim, D.H. *Synthesis* **2006**, 603. https://doi.org/10.1055/s-2006-926294
44. Becke, A.D. *J. Chem. Phys.* **1993**, *98*, 5648. https://doi.org/10.1063/1.464913
45. Lee, C.; Yang, W.; Parr, R.G. *Phys. Rev. B: Condens. Matter Mater. Phys.* **1988**, *37*, 785. https://doi.org/10.1103/PhysRevB.37.785
46. Miehlich, B.; Savin, A.; Stoll, H.; Preuss, H. *Chem. Phys. Lett.* **1989**, *157*, 200. https://doi.org/10.1016/0009-2614(89)87234-3
47. Orio, M.; Pantazis, D.A.; Neese, F. *Photosynth. Res.* **2009**, *102*, 443. https://doi.org/10.1007/s11120-009-9404-8
48. Frisch, M.J.; Trucks, G.W.; Schlegel, H.B.; Scuseria, G.E.; Robb, M.A.; Cheeseman, J.R. Gaussian 09, **2009**, Gaussian, Inc., Wallingford, CT, USA.
49. Dennington, R.D.; Keith, T.A.; Millam, J.M. GaussView 5.0. 8. **2008**. *Gaussian Inc*.